JKAU: Mar. Sci., **Vol. 18,** pp: 121-148 (2007A.D. /1428 A.H.)

Environmental Impact Assessment of Na'ama Bay Fountain, Sharm El'Shiekh, Southern Sinai, Egypt

Ebtessam E.E. Mohamed, Ali I. Beltagy, Khaled A. Moussa and **Gerges F. Soliman**

National Institute of Oceanography and Fisheries
Kayet Bey, Alexandria, Egypt

Abstract. A project for the installation and operation of a floating fountain in Na'ama bay, Sharm El'Shiekh, Southern Sinai is proposed. To fulfill the requirements of the project, an environmental impact assessment (EIA) study was conducted to identify and assess potential impacts of the project on environment of the bay.

In the framework of the project, the following activities were conducted:

1- Bathymetric Survey
2- Bottom Survey
3- Current and tide measurements
4- Meteorological data were obtained
5- Wave refraction and diffraction models were constructed and applied
6- Current models were constructed and applied, and
7- Modeling of water suction and flow by fountain

From these activities, the following conclusions were reached:

The proposed site is suitable for the installation of the fountain since the energy transmitted by waves to different parts of the bay is very small. However, for safety reasons and because of the slope of the bottom and the area defined for transmission of deeper waves into the bay, another location is proposed.The results of the EIA study conducted for the project of installing and operating a floating fountain in Na'ama bay area indicated that the project might have minor potential impacts on the environment in the bay. These impacts will bee mostly limited to the installation phase and will be transient and localized in nature as well. However, it is expected that the project will also significantly contribute to the attractiveness of the area, thus promoting tourism and recreational activities, employment and income in the area.

Introduction

The Gulf of Aqaba is one of the two narrow northward extensions of the Red Sea. It is 180 km long, 14-26 km wide and is located between the desert of Sinai to the west and Jordan and Saudi Arabia to the east (Morcos, 1970).

Na'ama bay is a semi-circular basin surrounded by two plateaus. The beach area is occupied by different tourist installations. The beach slope is relatively steep (12%) in the area following the tidal march. Seawards, the depth changes at a larger rate to 10, 20 and 30 meters in a distance less than 500 meters; *i.e.* slope of 6%. However, the change is not regular and several sub-water depressions are present (NIOF, 1993 & 2004).

The section between the two heads on both sides of the Bay show a submarine channel-shape, which indicates that the bay may have been an extension of a terrestrial valley.

The beach area is relatively wide and represented by a dry sabkha zone separated from the water line by a sandy ridge.

Landwards, a walking road that connects all the tourist facilities on the beach of the Bay exists. This road is followed by the main hotel facilities, which occupy about 200m between the beach and the main road of Sharm El-Sheikh.

The beach face is characterized by a high slope so that the intertidal zone is narrow. The beach slope ends up with a berm, where the backshore zone slopes landward forming some patches of salt layers resulting from evaporation. However, the surface of the backshore zone has wet sediments (NIOF., 2004).

Seaward from the shoreline, the bottom is sandy or sandy with some patches of coral reefs. The subtidal and intertidal sediments are both made of quartz and feldspar grains in addition to some carbonaceous materials. The subtidal zone had moderately sorted coarse sands, while the intertidal zone had poorly sorted fine sands (NIOF, 2004).

Environmental Condition

1- Climatic Condition

The climate of the region is subtropical; *i.e.* merely arid. In winter, it is generally cold intervened with short mild periods. In spring, the weather is changeable characterized by frequent Khamasin waves of

varying intensity and duration. The stable weather prevailing in summer is mild. In autumn, the weather is mild with heat waves (NIOF., 2005).

The minimum air temperature is around 9^{o} C occurs in January in winter. The temperature starts to rise in February. In summer, it reaches its maximum around 32^{o} C in July. The average annual range is about 23.3^{o} C, while the diurnal range may exceed 20^{o} C in summer.

Rainfall is scarce with great variability in winter.

Moderate N-NNE and NNW wind dominates the area allover most of the year. This may change to SE for short periods. Such winds might be strong enough to generate moderate water waves. The Khamasin (westerly wind) blows often in spring and autumn, which is mostly hot and sandy. Wind speeds more than 20 knots rarely occur and blow from N-NNE and WNW (Anon, 1980).

Data and Analysis

A hydrographic survey was conducted to collect and furnish data and information required for the optimization of design and implementation criteria of the Na'ama Bay Fountain installation. Fieldwork was required to collect data for:

1- Bathymetry of the proposed area,

2- Records of current speeds and directions by current-meter of Aanderaa-RCM7 in the proposed location of the future installation Point A (Fig. 1) for the period of field work,

3- Records of tide using a continuous-record water level recorder of the Aandera-WLR type in the proposed location of the future installation Point A for the period of field work,

4- Meteorological data required for hydrodynamic modeling of the area were acquired from records of Ras Nasrani International Airport.

Results and Discussion

1- Beach Area

The beach area is relatively wide and represented by a dry sabkha separated from the water line by a sandy ridge. Landwards, a walking road that connects all the tourist facilities on the beach of the Bay exists.

This road is followed by the main hotel facilities, which occupy about 200m between the beach and the main road of Sharm El-Sheikh.

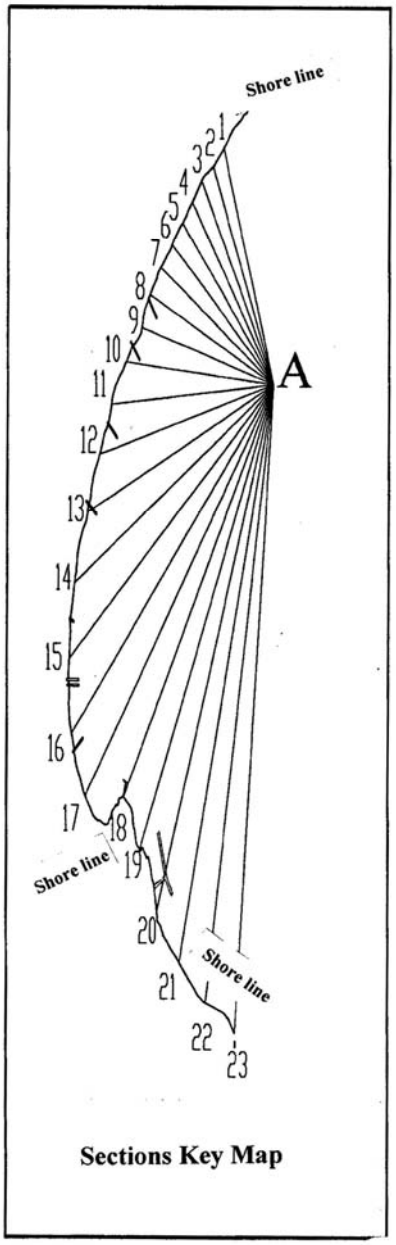

Fig. 1. Detailed Bathymetric Survey Gird.

2- Bottom Topography

The bottom depth profiles of the detailed bathymetric survey are shown in Fig.1 which is related to the low water level. The bottom depths are corrected to the low water depth, mean water level and to high water level.

The bathymetric contour map of the survey area is shown in Fig. 2. This map shows that bottom at the proposed location of installation (point A) is made of a quite prominent high or plateau (10m depth) relative to the surrounding much deeper bottom (> 12 meter depth).

Aside from the fact that depths increase in a general seaward direction in the area, local and major variations in bottom gradients are most easily discernible from the figure. Thus, the northern part of the area is characterized by much smoother and gentle bottom depth gradients with maximum depths of about 25 meters at the eastern end of this area. In the southern part of the area, depths and depths gradients increase at almost double the rate found in the northern part. This pattern might be a reflection of differences in controls affecting the two parts of the bay with tectonism being the main shaping factor at south, and sedimentological processes as the dominant shaping ones at north.

3- Current

The general current pattern in the open sea off Na'ama bay shows variations on different temporal scales according to variations in wind regime. The current outside the bay is mainly affected by the local wind, the mean sea level and pressure gradient due to changes in temperature and salinity.

Due to shallowness of the area and small scale of its dimensions current speeds are reduced greatly near the shores. This is proved by records made at different localities in the Bay, whish showed speeds between 2.0 and 8.0 cm/sec.. Accordingly, it is expected to find a stable coastal configuration.

Percentage frequency of current recorded in Na'ama bay around the proposed sit and during ebb and neap is calculated and represented in Fig. 3.

Due to the lack of current measurements, a mathematical model for homogeneous basin which developed by Hansen (1962), and applied by

Soliman (1995) using different cases with a wind stress of 1.0 dyne/cm^2 and a boundary condition of different inflow values 10.0 and 30.0 cm/sec from the right or left of the Bay intrance. The results obtained are represented in Fig. 4-7.

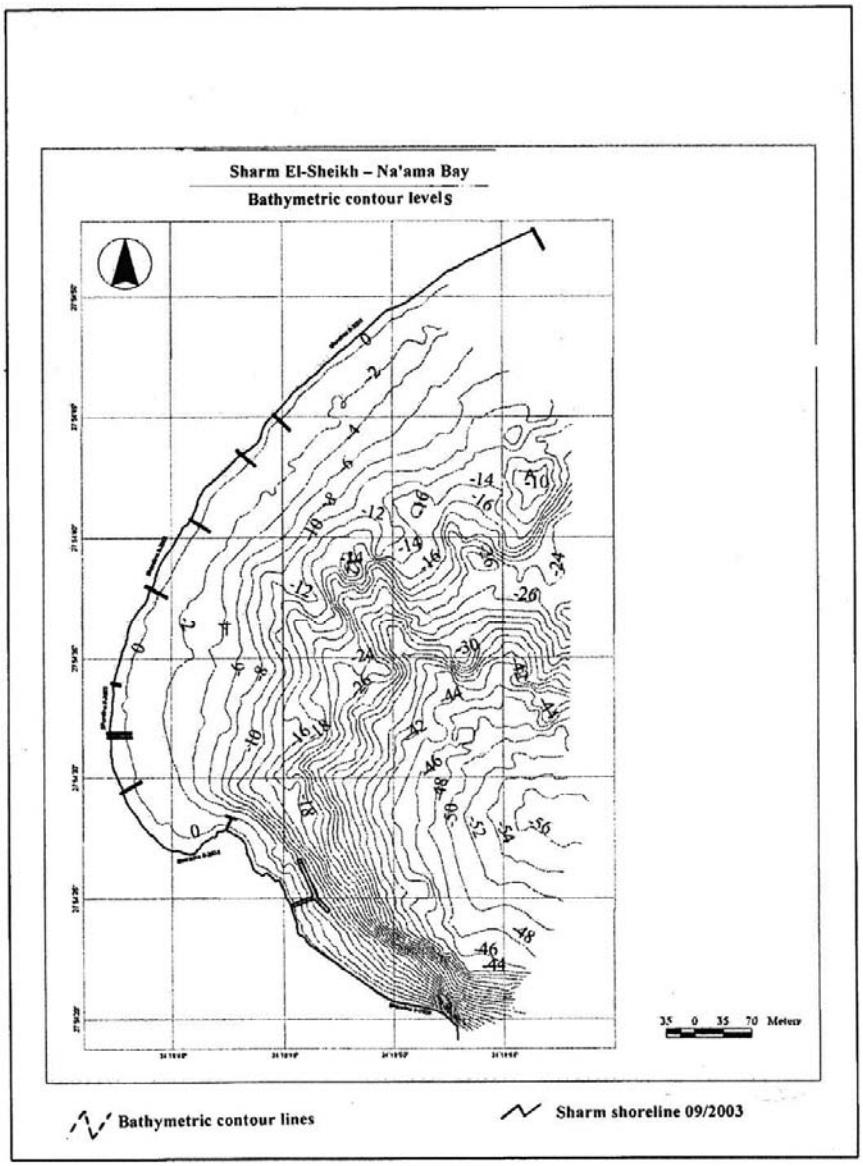

Fig. 2. Bathymetric contour map of the survey area relative to low water level.

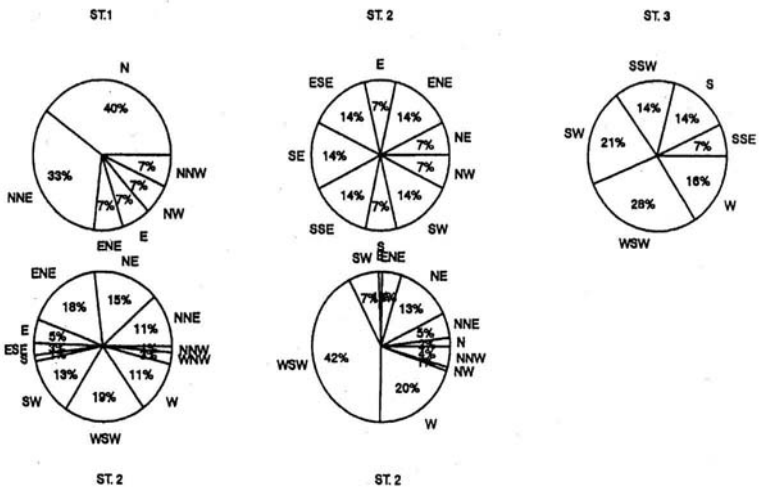

Fig. 3. Percentage frequency of current distribution in Na'ama bay.

4- Waves

Waves are generally generated by winds. They have irregular and complex shapes because of the interaction between individual waves. Energy from wind is transferred to the sea surface generating short and intermediate waves. These winds – induced waves depend mainly on wind speed, direction, fetch and duration. The wave characteristics due to wind action for different durations and fetches using different equations as in Tables 1 & 2, and by using predicting wave diagram and given in Table 3. Energy impacts on the structure fixing the fountain to the bottom were calculated and found to be very small in magnitude.

Although the N-NE winds are dominated in the area under study, the most effective winds distribute strongly the sea surface, as well as those blowing from the S-SE directions. The waves coming along the Gulf of Aqaba from the N, due to N-NE winds are dissipated upon leaving the strait of Tiran, and hence the area under investigation is slightly affected by such waves. In addition, the bathymetric map of the area (Fig. 2) indicates the existence of submerged cell of about 35m at the entrance of Na'ama bay. The existence of such cell acts as a barrier, reflecting the waves before entering the bay. Therefore it is expected to find damped waves of wave height less than 1.0m, within the bay waves penetrate the bay will suffer from diffraction (Fig. 9) as spreading inside the bay, which, reduces greatly the wave energy, occurring from the open sea.

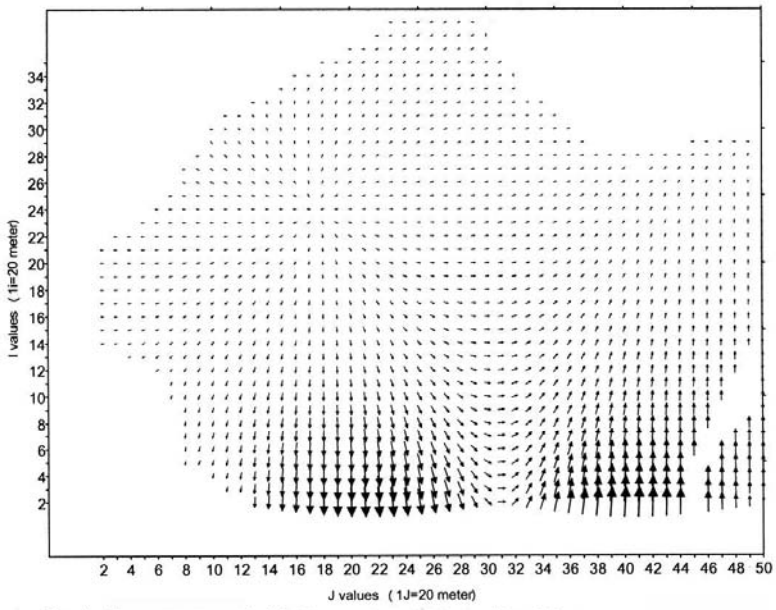

Fig. 4. Current pattern inside Na'ama bay, inflow right side, outflow left side with maximum flow range 10 cm/sec.

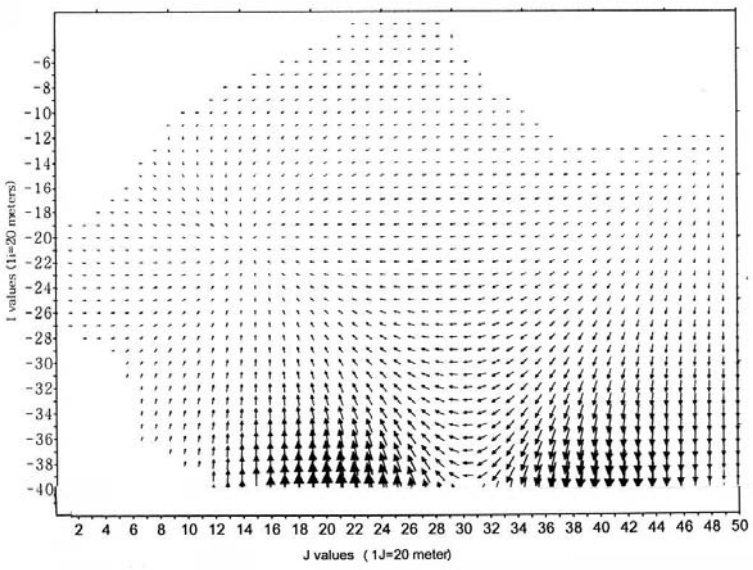

Fig. 5. Current pattern inside Na'ama bay, inflow left side, outflow right side with maximum flow range 10 cm/sec.

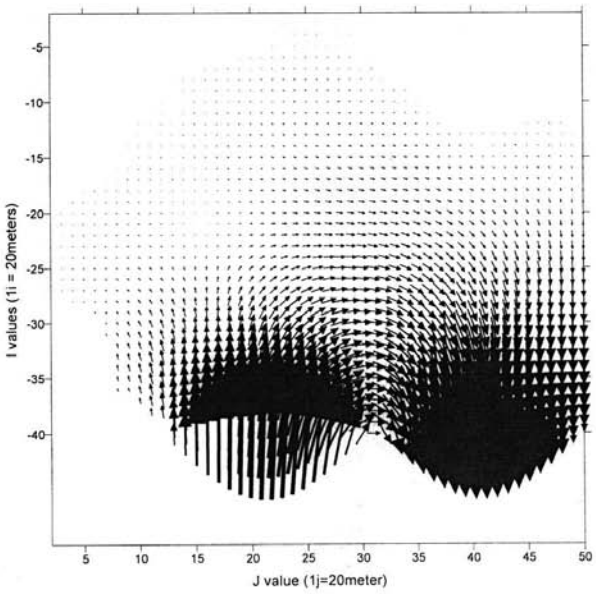

Fig. 6. Current pattern inside Na'ama bay, inflow left side, outflow right side with maximum flow range 30 cm/sec.

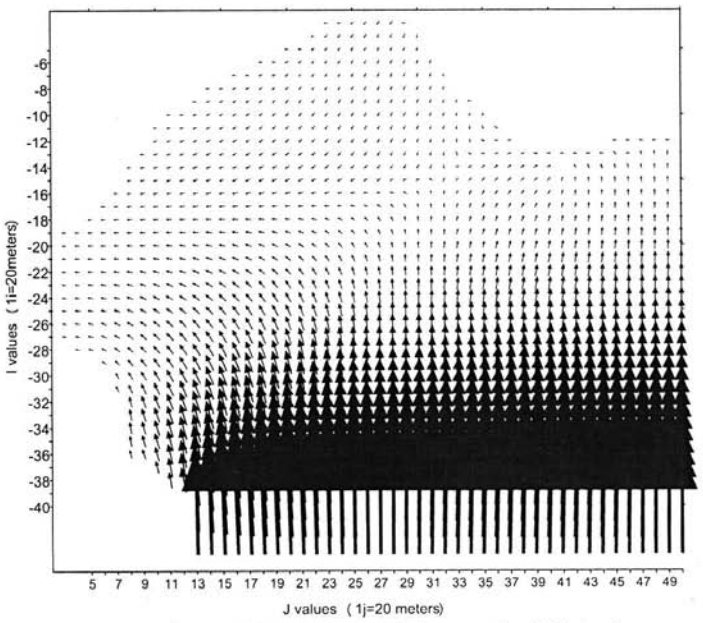

Fig. 7. Current pattern inside Na'ama bay, inflow over the whole opening similar to the tidal current with maximum flow of 30 cm/sec.

Table 1. Wave characteristics according to plane wave model equations (P.M.).

Wind speed range (Knots)	Specified wind speed (knots)	H_{av} (m)	$H_{1/3}$ (m)	$T_{1/3}$ (sec)	$H_{1/10}$ (m)
	Minimum (1.0)		0.027	0.826	
1.0 – 10.0	Maximum (10.0)		0.676	4.108	
	Average (5.0)		0.169	2.054	
	Minimum (11.0)	0.53	0.82	4.5	1.06
11 _ 20	Maximum (20.0)	1.76	2.70	8.2	3.48
	Average (15.0)	0.98	1.50	6.2	1.94
	Minimum (21.0)	1.94	2.98	8.6	3.84
21 – 29	Maximum (29.0)	3.70	5.69	11.9	7.30
	Average (25.0)	2.75	4.23	10.3	5.46

$H_{1/3}= 0.025 * U^2$
$T_{1/3}= 0.79 *U_{10}$

Table 2. Wave characteristics according to JONSWAP Model.

Wind speed range (Knots)	Specified wind speed (knots)	H_{av} (m)	$H_{1/3}$ (m)	$T_{1/3}$ (sec)	$H_{1/10}$ (m)
	Minimum (1.0)		0.232	2.295	
1.0 – 10.0	Maximum (10.0)		1.62	3.72	
	Average (5.0)		0.581	3.022	
	Minimum (11.0)	0.83	1.28	3.8	1.65
11 – 20	Maximum (20.0)	1.50	2.30	4.6	2.96
	Average (15.0)	1.13	1.74	4.2	2.25
	Minimum (21.0)	1.59	2.44	4.6	3.15
21 – 29	Maximum (29.0)	2.19	3.37	5.1	4.35
	Average (25.0)	1.89	2.91	4.9	3.75

$H_{1/3}= 0.00051 * U_{10} *F^{0.5}$
$T_{1/3}= 0.059 *(U_{10} *F)^{0.03}$
Fetch considered to the north wind = 192km.

Table 3. Wave characteristics obtained from predicting wave diagram.

Wind speed (knots)	Specific wind speed (knots)	Fetch (192 km)															
						6 hours duration				12 hours duration				18 hours duration			
		$H_{1/3}$	$T_{1/3}$	Havr	$H_{1/10}$	$H_{1/3}$	$T_{1/3}$	Havr	$H_{1/10}$	$H_{1/3}$	$T_{1/3}$	Havr	$T_{1/10}$	$H_{1/3}$	$T_{1/3}$	Havr	$T_{1/10}$
	If fetch <100km	<0.66				<0.66	3.4			0.66	4.2		0.76	5			
1-10																	
	If fetch > 100km	<0.99															
	Min	0.86	5	0.56	1.11	0.2	3.7	0.13	0.26	0.83	4.6	0.54	1.06	0.89	5	.58	1.15
11-20	Aver	1.49	6.05	0.97	1.92	0.99	4.6	0.64	1.28	1.39	5.7	0.9	1.79	1.58	6.6	1.03	2.04
	Max	2.08	7	1.35	2.68	1.58	5.6	1.3	2.04	2.11	6.9	1.37	2.72	2.57	7.8	1.67	3.32
	Min	2.34	7.2	1.52	3.02	1.75	5.8	1.14	2.26	2.15	7.1	1.39	2.77	2.71	8	1.76	3.49
21-29	Aver	2.97	7.85	1.93	3.83	2.28	6.5	1.48	2.94	3.04	8	1.97	3.92	3.99	9.1	2.6	5.07
	Max	3.63	8.5	2.36	4.68	274	7.2	1.78	3.53	3.91	8.8	2.54	5.04	4.62	10	3	5.96

Although the N-NE winds are dominated in the area under study, the most effective winds distribute strongly the sea surface, as well as those blowing from the S-SE directions. The waves coming along the Gulf of Aqaba from the N, due to N-NE winds, are dissipated upon leaving the strait of Tiran, and hence the area under investigation is slightly affected by such waves. In addition, the bathymetric map of the area (Fig. 2) indicates the existence of submerged cell of about 35m at the entrance of Na'ama bay. The existence of such cell acts as a barrier, reflecting the waves before entering the bay. Therefore it is expected to find damped waves of wave height less than 1.0m, within the bay the waves penetrate the bay will suffer from diffraction (Fig. 9) as spreading inside the bay, which, reduces greatly the wave energy, occurring from the open sea.

As the waves propagate towards the shore, they dissipate a large part of their energy in the near shore zone. Wave momentum and energy fluxes are responsible for generating long shore currents and sediment transport. Wave energy may be dissipated through turbulent fluid motion induced by wave breaking and bottom friction. These phenomena have great influence in the stability of the coastal zones. Thus, any coastal task

depends greatly on the understanding of the wave pattern and fluid motion under waves.

The statistical summaries for the wave field of 1 and 100 year return period according to the dominating wind direction and speed are given in Tables 4 & 5. The most effective winds are those blowing from N, NE with speed range of 11-29knots. Meteorological observations at Ras Nusrani (Sharm El-Shikh air port) did not indicate the presence of any wind with speed more then 30 knots. In other nearby meteorological stations such as El-Tor, Hurghada and East Zeit, speeds of more than 40 knots were recorded in a very few cases. However, the waves we deal with have speed of 29 knots as maximum speed. Refraction diagram was drawn for waves with wave length of about 56.0m and period 6.0 second is given in Fig. 8.

Table 4. Statistical summary for the wave field of 1year return period.

Wind speed range (knots)	Specific wind speed (knots	Maximum wind duration (hour)	Mean wave		Significant wave		Maximum wave	
			Height (m)	Period (sec)	Height (m)	Period (sec)	Height (m)	Period (sec)
11-20	Minimum	6	0.125	3.0	0.2	3.7	0.35	5.9
	Maximum		0.99	4.5	1.58	5.6	2.78	8.9
	Average		0.62	3.7	0.99	4.6	1.74	7.3
	Minimum	12	0.52	3.7	0.83	4.6	1.46	7.3
	Maximum		1.32	5.5	2.11	6.9	3.71	10.9
	Average		0.87	4.6	1.39	5.7	2.45	9.0
	Minimum	18	0.56	4.0	0.89	5.0	1.57	7.9
	Maximum		1.61	6.3	2.57	7.8	4.52	12.4
	Average		0.99	5.3	1.58	6.6	2.78	10.5
21-29	Minimum	6	1.10	4.7	1.75	5.8	3.08	9.2
	Maximum		1.72	5.8	2.74	7.2	4.82	11.4
	Average		1.43	5.2	2.28	6.5	4.01	10.3
	Minimum	12	1.35	5.7	2.15	7.1	3.78	11.3
	Maximum		2.45	7.1	3.91	8.8	6.88	14.0
	Average		1.91	6.4	3.04	8.0	5.35	12.7.03
	Minimum	18	1.70	6.4	2.71	8.0	4.77	12.7.03
	Maximum		2.90	8.0	4.62	10.0	8.13	15.9
	Average		2.50	7.3	3.99	9.1	7.02	14.4

Table 5. Statistical summary for the wave field of 100 year return period.

Wind speed range (knots)	Specific wind speed (knots	Maximum wind duration (hour)	Mean wave		Significant wave		Maximum wave	
			Height (m)	Period (sec)	Height (m)	Period (sec)	Height (m)	Period (sec)
11-20	Minimum	6	0.199	3.8	0.317	4.8	0.558	5.5
	Maximum		1.571	5.9	2.506	7.3	4.411	8.4
	Average		0.984	4.8	1.570	6.0	2.763	6.9
	Minimum	12	0.825	4.8	1.316	6.0	2.316	6.9
	Maximum		2.098	7.2	3.346	9.0	5.889	10.4
	Average		1.382	5.9	2.205	7.4	3.881	8.5
	Minimum	18	0.885	5.2	1.412	6.5	2.485	7.5
	Maximum		2.555	8.2	4.076	10.2	7.174	11.7
	Average		1.571	6.9	2.506	8.6	4.411	9.9
`21-29	Minimum	6	1.74	6.1	2.776	7.6	4.886	8.7
	Maximum		2.725	7.5	4.346	9.4	7.649	10.8
	Average		2.267	6.8	3.616	8.5	6.364	9.8
	Minimum	12	2.138	7.5	3.410	9.3	6.002	10.7
	Maximum		3.888	9.2	6.201	11.5	10.914	13.2
	Average		3.023	8.3	4.821	10.4	8.485	12.0
	Minimum	18	2.695	8.3	4.298	10.4	7.564	12.0
	Maximum		4.594	10.4	7.327	13.0	12.896	15.0
	Average		3.967	9.5	6.328	11.9	11.137	13.7

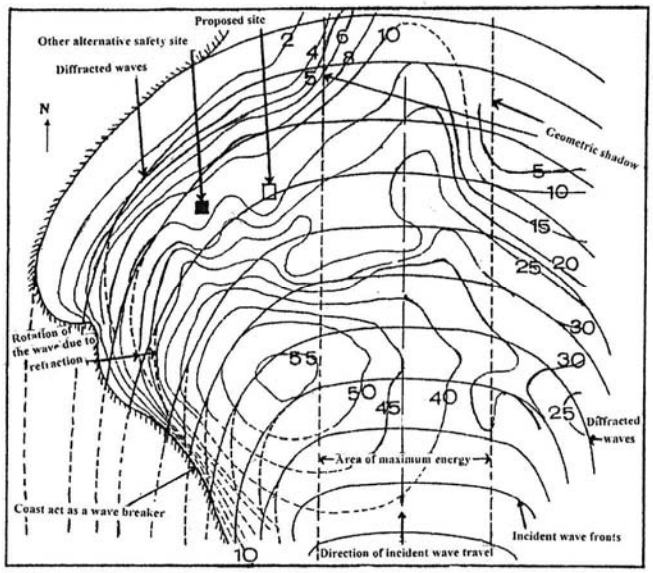

Fig. 8. Diffraction diagram of waves in Na'ama bay.

5- Modeling of Water Flow

In case of installing the fountain in the bay many models must be applied to know the effect of water flow from and into the bay.

5-1 Water Intake Model

It is often desirable to find the equation describing the streamlines of a flow in the bay. With cylindrical coordinates, for a flow symmetrical with respect to the z axis, v=0 and u and w are functions of r and z only. Since the flow is identical in all meridian planes. It is necessary to study only the flow in one meridian plane at a constant Θ (Douglas *et al*., 1992)

For an incompressible flow with v=o the equation of continuity are:

$$\frac{\delta ur}{\delta r}+\frac{\delta wr}{\delta z}=0.0$$

Thus it is Possible to describe the flow with a function ψ (r,z,t) defined by

$$Ur = -\delta\psi/\delta z$$
$$Wr = \delta\psi/\delta r$$

The flow described by such a function will automatically satisfy the equation of continuity:

$$\frac{\delta ur}{\delta r}+\frac{\delta wr}{\delta z}=-\frac{\delta^2\Psi}{\delta r\delta z}+\frac{\delta^2\psi}{\delta z\delta r}$$

This function ψ is known as the Stockes's stream function for axially symmetric incompressible flow:

In this study the stream function, which gives the pattern of flow is

$$\psi=\frac{1}{2ur^2}+Q\frac{(1-\frac{z}{\sqrt{r2+z2}})}{4\Pi}$$

Where:

U is the field velocity.

Q discharge of water (650m^3/h).

From the above stream function :

$$U = \frac{Qr}{4\Pi (r^2 + z^2)^{3/2}}$$

$$w = u + \frac{Qz}{4\Pi (r^2 + z^2)^{3/2}}$$

Applying the above equations the stream flow deduced when 650 m^3 of water is pumped within l hour is represented in Fig. 9.

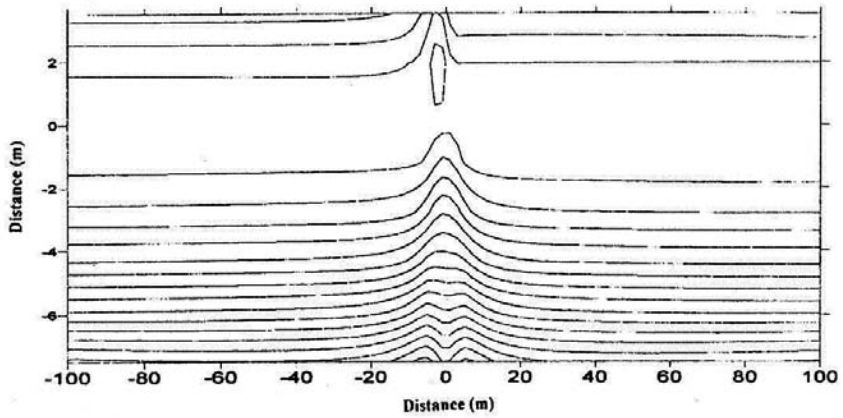

Fig. 9. Pattern of stream flow.

Also, the velocity field obtained in the site of pumping water is given in Fig. 10. It is obvious that the very near area to the pump is affected by the suction of water where the velocity of water approaches 30cm/sec. These values reduced to be near the ambient speed within 20m approximately.

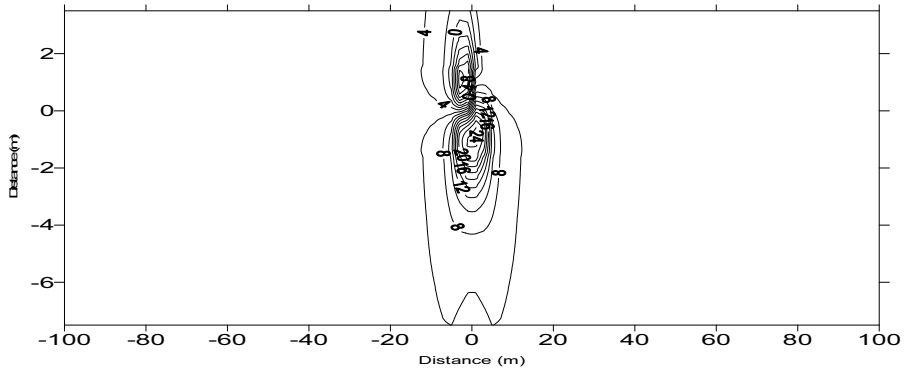

Fig. 10. Velocity fields (cm/sec) generated by suction pumps in Na'ama bay.

From the above two figures, it is evident that the effects of water suction will be limited to areas very near to sea inlet boxes where the velocity of water approaches 30 cm/sec with these velocities dimensioning to near ambient current speeds of 6 cm/sec, within horizontal distances of about 20meter on either side.

5-2 Model of Water Outflow

The description of the motion of water droplets that fly from fountain is discussed by many authors among them Mahesh (1996), Foglemen *et al*. (2001), Agrawal and Prasad (2003), Muppidi and Mahesh (2004), Muppidi and Mahesh (2005) and Anon (2005).

5-2-1 Position and Displacement

Considering the particles move in XY plane and introduction of a Cartesian coordinate system that contains an origin and X and Y axis. The change in particle position from point P at time t_1 to point Q at time t_2 is known as the displacement vector

$\Delta r = r_Q - r_P$ (1) as shown in Fig. 11.

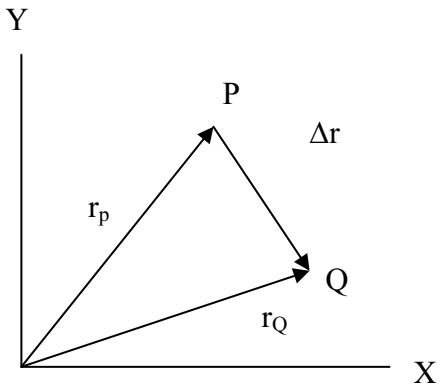

Fig. 11. The particle moving in XY plane.

5-2-2 Velocity and Acceleration

Using equation (1) for the particle displacement, the average velocity V_{av} over the finite time interval from t to t+Δt is accordingly defined by:

$$V_{av} = \frac{r(t+\Delta t) - r(t)}{\Delta t} = \frac{\Delta r}{\Delta t} \qquad (2)$$

As the time Δt tends towards zero, the instantaneous velocity v(t) is given by the following equation (3):

$$V(t) = \lim \frac{r(t+\Delta t) - r(t)}{\Delta t} = \frac{dr}{dt} \tag{3}$$

Then the velocity vector can be given from the following equations:

$$V = \frac{d}{dt} r(t) = \frac{d}{dt} \{ x(t) + y(t) \tag{4}$$

$$= \frac{dx}{dt} i + \frac{dy}{dt} J \tag{5}$$

Equation (5) can be written in the form

$$\bar{V} = \bar{V_x} + \bar{V_y} \tag{6}$$

The magnitude of the velocity vector V is equal to

$$V = \sqrt{v_x^2 + v_y^2} \tag{7}$$

The angle θ that the vector velocity make with the X axis is determined by:

$$\tan\theta = \frac{v_x}{v_y} \tag{8}$$

The acceleration describes how rapidly velocity changes with time. For a finite time interval Δt, the average acceleration is defined as:

$$a_{av} = \frac{v(t+\Delta t) - v(t)}{\Delta t} = \frac{\Delta v}{\Delta t} \tag{9}$$

and the components of the acceleration vector are:

$$a_x = \frac{dv_x}{dt} = \frac{d^2x}{d^2t} \tag{10}$$

$$a_y = \frac{dv_y}{dt} = \frac{d^2y}{d^2t} \tag{11}$$

5-2-3 Motion with constant Acceleration

The plane of motion is formed by the initial velocity vector and the acceleration vector. The plane of the motion is known as the XY plane. The x and y components of the position r and the velocity v in terms of constant acceleration components are:

$$x - component \quad of \quad \bar{r}: \qquad x = x_o + v_{ox}t + 0.5a_x t^2 \tag{12}$$

$$x - component \quad of \quad v: \qquad v_x = v_{ox} + a_x t \tag{13}$$

$$y - component \quad of \quad r: \qquad y = y_o + v_{oy}t + 0.5a_y t^2 \tag{12}$$

$$x - component \quad of \quad v: \qquad v_y = v_{oy} + a_y t \tag{13}$$

Here x_o and y_o are the components of $r = r_o$ at an initial time $t = 0$ and v_{ox} and v_{oy} are the components of $v = v_o$ at time $t = 0$. Together these quantities are the given initial conditions. These equations are known as the kinematic equations.

5-2-4 Projection Motion

In the absence of air resistance, the fountain water moves under the effect of gravity. Then the motion is with constant acceleration due to gravity, and this constant acceleration g has only a vertical component. The kinematics equations can be used to find the trajectory.

Suppose that the flow o water makes an angle θ with the x axis and initial velocity is v_o then the components of velocity are equal to:

$$v_{ox} = v_o \cos\theta_o \qquad and \qquad v_{oy} = v_o \sin\theta_o \tag{14}$$

The components of the acceleration are constant

$$a_x = 0 \qquad and \qquad a_y = -g \tag{15}$$

Applying the kinematic equations gives:

$$x = (v_o \cos\theta_o)t \tag{16}$$

$$y = (v_o \sin\theta_o)t - 0.5gt^2 \tag{17}$$

$$v_x = v_o \cos\theta_o \tag{18}$$

$$vy = v_o \sin\theta_o - gt \tag{19}$$

Then the trajectory of water flow can be found by plotting its height y versus its x-position. Both the *x* and *y* values are functions in time *t*. eliminating the time dependence from equations 16 & 17 we get:

$$t = \frac{x}{v_O \cos\theta_O} \tag{20}$$

$$y = (v_O \sin\theta_O)\frac{x}{v_O \cos\theta_O} - 0.5g\left[\frac{x}{v_O \cos\theta_O}\right]^2 \tag{21}$$

$$= (\tan\theta_O)x - \left[\frac{g}{2v_o^2 \cos^2\theta_O}\right]x^2$$

The coefficients of x and x^2 in equation (21) are both constants, so the trajectory has the form:

$$y = C_1x - C_2x^2 \tag{22}$$

The range R of the projectile is the value of the *x* when the projectile has returned to the beginning flow point *i.e.* y=0

Then:

$$Y=0=R(c_1 - c_2R) \tag{23}$$

Then:

$$R = \frac{c_1}{c_2} = \frac{v_o^2}{g}\sin 2\theta_O \tag{24}$$

The maximum range R_{max} is equal to:

$$R_{\max} = \frac{v_o^2}{g} \tag{25}$$

The total flight time is equal to:

$$T = \frac{2v_O}{g}\sin\theta_O \tag{26}$$

Also, the maximum height y_{max} =h is reached at time T/2 which is given from the following equation.

$$h = (v_O \sin\theta_O)\frac{2v_O}{2g}\sin\theta_O - 0.5g\left[\frac{2v_O}{2g}\sin\theta_O\right]^2 = v_o^2\frac{\sin^2\theta_O}{g} - gv_o^2\frac{\sin^2\theta_O}{2g^2}$$

$$= v_o^2\frac{\sin^2\theta_O}{2g} \qquad (27)$$

Applying the above system of equations to predict the maximum height (H_{max}) and the maximum range (R_{max}) and total time required to the jet to return back to the sea surface. Also these equations are used to obtain the corresponding values X and Y defining the trajectory of the water flow from the fountain.

Different alternatives are considered in this study:

6- Main Nozzle

Two alternatives are considered for water flow from the main nozzle as follows:

6-1 Alternative 1: Jet Height=123m & Θ=90^o

In this case if the angle (Θ) with the x axis = 90^o. Then the initial velocity V_o will be 49.1 m/sec, and the water flow down inside the fountain around its same position. This will take about 10 second.

6-2 Alternative 2: Jet Height=123m & Θ=5-80^o

The calculated values of V_o, H_{max}, R_{max}, and T_{max}. are given the following table:

Calculated V_o, R_{max}, and T_{max}, with different angles at a jet height of 123m .

THETA	VO	R_{MAX}	T_{MAX}
80	49.8573	86.48476	10.02137
70	52.251	178.8632	10.02218
60	56.69568	283.918	10.02282
50	64.40954	416.8423	10.07247
40	76.38588	586.4008	10.02374
30	98.1998	852.3763	10.02404
20	143.5585	1352.212	10.02426
10	282.755	2791.348	10.02438
5	563.3582	5625.826	10.02441

From this table, it is evident any deviation of the main jet from $\Theta=90^o$ will result in lateral spread that will reach far inland or may fall in the shallow water near the beach causing undesirable water and sediment disturbances. Accordingly, the main jet should be directed at $\Theta=90^o$ and not be allowed to spread outside the fountain structure.

6-3 Annulus

The calculated values of V_o, H_{max}, R_{max}, and T_{max}. for water jets with 25-meter heights are given in the following table:

Calculated V_o, R_{max}, and T_{max}, with different angles at a jet height of 25m.

THETA	V_0	R_{MAX}	T_{MAX}
90	22.1359	0.0	4.51753
80	22.4774	17.57819	4.517981
70	23.556	36.35256	4.518236
60	25.56	57.70516	4.51857
50	28.896	83.8971	4.518805
40	34.437	119.1843	4.518998
30	44.2719	173.2473	4.51919
20	64.4758	272.7598	4.50215
10	127.4758	567.3469	4.519339
5	253.981	1143.456	4.519345

From this table, it is evident that the maximum angle for water jets from the annulus is 70^o as water at this angle covers a circle with a radius almost matching the locations of buoys marking the locations of anchor about the fountain structure (35m). Smaller angles will cause water falling in much larger circles causing great turbulence in water and even reaching bottom sediments near the shore and causing major disturbances for all activities in the bay area.

7- Disturbances by Falling Water

Since water is incompressible, the principle of conservation of mass implies compensation of any random movement of small mass of water within the fluid medium by an opposite motion, thus illustrating the swirling – flow aspect of turbulence. An immediate effect of turbulent

eddies is that they cause rapid propagation in all directions of the various properties associated with liquid particles. The maximum depth water from jets might penetrate into the seawater column due to falling under the effect of gravity can be calculated using the following equation (Bonazountas, 1987 & Mohamed *et al*., 1997):

$$Y^{\max} = 2.84(Y'q)^{1/3}\{(g/\rho)\frac{d\rho}{dy}\}^{-1/2}$$

where

$Y' = g\,\Delta\rho/\rho$

ρ = the density of falling water

$\Delta\rho$ = the density difference between the falling water and the ambient water

g = is the gravitational acceleration

q = volume of falling water per unit area

Applying the above formula on the falling water from different nozzle diameters (1, 2, 2.5, 3, 4 and 5cm) and a maximum jet height is 25m would give the following results corresponding to each nozzle diameter:

Nozzles diameter = 1cm

Theta	v_o	R_{max}	$q(m^3)$	Y_{max} (m)
90	22.1359	49.9998	0.001739	3.772565
80	22.4774	51.554	0.001766	3.791865
70	23.556	56.6209	0.001851	3.851566
60	25.56	66.6646	0.002008	3.957819
50	28.896	85.2019	0.00227	4.122997
40	34.437	121.0109	0.002706	4.371257
30	44.2719	200	0.003479	4.753028
20	64.4758	424.1968	0.005066	5.387506
10	127.4758	1658.171	0.010016	6.761685
5	253.981	6582.28	0.019956	8.508169

Nozzles diameter =2.0cm

Theta	v_o	R_{max}	$q(m^3)$	Y_{max} (m)
90	22.1359	49.9998	0.006957	5.988297
80	22.4774	51.554	0.007064	6.018932
70	23.556	56.6209	0.007403	6.113697
60	25.56	66.6646	0.008033	6.282355
50	28.896	85.2019	0.009082	6.544548
40	34.437	121.0109	0.010823	6.938618
30	44.2719	200	0.013914	7.544613
20	64.4758	424.1968	0.020264	8.551738
10	127.4758	1658.171	0.040064	10.73301
5	253.981	6582.28	0.079823	13.50525

Nozzles diameter = 2.5cm

Theta	v_o	R_{max}	$q(m^3)$	Y_{max} (m)
90	22.1359	49.9998	0.01087	6.9487
80	22.4774	51.554	0.011038	6.984248
70	23.556	56.6209	0.011568	7.094211
60	25.56	66.6646	0.012552	7.289919
50	28.896	85.2019	0.01419	7.594162
40	34.437	121.0109	0.016911	8.051433
30	44.2719	200	0.021741	8.754618
20	64.4758	424.1968	0.031662	9.923265
10	127.4758	1658.171	0.0626	12.45437
5	253.981	6582.28	0.124723	15.67122

Nozzles diameter = 3.0cm

Theta	v_o	R_{max}	$q(m^3)$	Y_{max} (m)
90	22.1359	49.9998	0.015653	7.846677
80	22.4774	51.554	0.015895	7.886819
70	23.556	56.6209	0.016657	8.010993
60	25.56	66.6646	0.018075	8.231992
50	28.896	85.2019	0.020434	8.575552
40	34.437	121.0109	0.024352	9.091916
30	44.2719	200	0.031307	9.885973
20	64.4758	424.1968	0.045594	11.20564
10	127.4758	1658.171	0.090144	14.06384
5	253.981	6582.28	0.179601	17.69641

Nozzles diameter =4.0cm

Theta	v_o	R_{max}	$q(m^3)$	Y_{max} (m)
90	22.1359	49.9998	0.027828	9.50539
80	22.4774	51.554	0.028257	9.554017
70	23.556	56.6209	0.029613	9.70444
60	25.56	66.6646	0.032133	9.972156
50	28.896	85.2019	0.036326	10.38834
40	34.437	121.0109	0.043292	11.01386
30	44.2719	200	0.055656	11.97577
20	64.4758	424.1968	0.081055	13.57441
10	127.4758	1658.171	0.160255	17.0368
5	253.981	6582.28	0.31929	21.43726

Nozzles diameter = 5.0cm

Theta	v_o	R_{max}	$q(m^3)$	Y_{max} (m)
90	22.1359	49.9998	0.043481	11.02986
80	22.4774	51.554	0.044152	11.08629
70	23.556	56.6209	0.046271	11.26084
60	25.56	66.6646	0.050207	11.57149
50	28.896	85.2019	0.05676	12.05442
40	34.437	121.0109	0.067644	12.78026
30	44.2719	200	0.086963	13.89645
20	64.4758	424.1968	0.126649	15.75147
10	127.4758	1658.171	0.250399	19.76917
5	253.981	6582.28	0.498891	24.87537

Based on above results, diameter of the annulus nozzles can be selected as not to exceed 2.5 cm.

On the other hand, floating units disperse water through the air, increasing droplet surface area and dissolved oxygen. Another benefit is increased circulation that gets dissolved oxygen where it will do some good. Circulation can break up layers of thermal stratification and reduce fish kills from seasonal pond thermal inversion. Also, increased dissolved oxygen will help aquatic life and aerobic bacteria that decompose sludge while increased circulation can separate algae from food sources.

Conclusion

A project for the installation and operation of a floating fountain in Na'ama bay, Sharm El'Shiekh, Southern Sinai is proposed. The project

consists of mooring a pontoon equipped with necessary equipment for operating an electrically operated floating fountain at a location with a 12-meter depth in the bay. The floating fountain system will be powered and operated through cables connected to onshore transformer and control panel.

To fulfill the requirements of the project, an environmental impact assessment (EIA) study was conducted to identify and assess potential impacts of the project on environment of the bay and propose adequate mitigation measures and environmental management plan for the project.

The results of the EIA study conducted for the project of installing and operating a floating fountain in Na'ama Bay area indicated that the project might have minor potential impacts on environment in the Bay. These impacts will be mostly limited to the installation phase and are transient and localized in nature as well.

However, it is expected that the project will also significantly contribute to the attractiveness of the area, thus promoting tourism and recreational activities, employment and income in the area.

Based on the findings of the study, it is suggested that the project can be implemented as long as the proposed environmental management plan is strictly applied and followed under the guidance and supervision of the Protectorates Division of the Egyptian Environmental Affairs Agency.

References

Anon., (1980) *Red Sea and Gulf of Aden Pilot*, Twelfth Edition, The Hydrographer of the navy.

Anon., (2005) *Motion in Two and Three Dimensions* (chapter 3). www.u.washington.edu/research/*seal/pubfiles/masters thesis fumin.doc*.

Agrawal, A. and **Prasad, A. K.** (2003) Integral solution for the mean flow profiles of turbulent jets, plumes, and wakes, *J. Fluids Engineering,* **125**: 813-822.

Bonazunntas, M. (1987) *Training Course in Modeling Outfall and Coastal Water Quality*, Athens, Greece.

Douglas, J.F., Gasiorex, J.M. and **Swaffield, J.A.** (1992) *Fluid Mechanics*, Longman Singapore Publishers, 746 p.

Mohamed, E.E., Abass, M.M., Said, M.A. and **Beltagy, A.I., (**1997) Environmental impact assessment of industrial development in the Suez Bay area of water and air quality, *Inter. J. Environmental Studies,* **53**:275-298.

Fogleman, M.A., Fawcett, M.J. and **Solomon, T.H.** (2001) Lagrangian chaos and correlated levy flights in an – Beltrami flow: Transient versus long term transport, *Physical Review,* **63**, 020101.

Hansen, W. (1962) Hydrodynamical methods applied to oceanographic problems, *Proc. of the Symposium on Mathematical – Hydrodynamical Methods of Physical Oceanography*, Mitt. Inst. Meeresk. Hamburg, No.1.

Krishnan, M. (1996) A Model for the onset of breakdown in an axisymmetric compressible vortex, *Phys. Fluids,* **8**(12): 3338-3345.

NIOF, (1993) *Environmental Impact Assessment of Construction of Artificial Lagoon in the Naema Bay Area for Oasis Hotel, Sharm El'Sheikh, South Sinai, Egypt.*

NIOF, (2004) *Na'ama Bay Fountain*, Final report

NIOF, (2005) *Environmental Impact Assessment of Naema Bay fountain project, Sharm El'Sheikh, South Sinai, Egypt.*

Mahesh, K. (1996) A model for the onset of breakdown in an axisymmetric compressible vortex, *Phys. Fluids,* **8**(12): 3338-3345.

Morcos, S.A. (1970) Physical and chemical oceanography of the Red Sea, *Oceanography & Marine Biology: An Ann. Rev*., **8**: 73-202.

Muppidi, S. and **Mahesh, K. (**2004) Study of trajectories of jets in cross flow using direct numerical simulations, *J. Fluide Mech*. (Under Publication).

Muppidi, S. and **Mahesh, K. (**2004) Direct numerical simulation of turbulent jets in cross flow. *American Inst. of Aeronautics and Astronautics*, 1-15.

Muppidi, S. and **Mahesh, K. (**2005) Study of trajectories of jets in a cross flow, *J. Fluid. Mech.,* (Under Publication).

Soliman, G.F. (1995) The influence of the last widening and deepening of the Suez Canal on its tidal motion, *Bull. Nat. Inst. Oceangr. & Fish., A.R.E*., **21**: 35-66.

الأثر البيئى لإنشاء نافورة بخليج نعمة – شرم الشيخ – جنوب سيناء – مصر

ابتسام السيد السيد محمد، و على إبراهيم بلتاجـــى، و خالد عبدالعال موســـى، و جرجس فهيم سليمان

المعهد القومى لعلوم البحار والمصايد

الإسكندرية – مصر

المستخلص. من أجل تثبيت نافورة عائمة بخليج نعمة تم التخطيط لعمل دراسات عن الآثار البيئية المترتبة عن عملية الإنشاء على خليج نعمة. وتضمنت تلك الدراسة المحاور التالية:

- عمل خريطة لطوبوغرافية القاع لمنطقة الدراسة.
- تحديد نوعية رسوبيات القاع.
- دراسة التيارات البحرية والمد والجزر بمنطقة الدراسة.
- تجميع بيانات عن الأرصاد الجوية وتحليلها.
- تطبيق نموذج رياضي عن انعكاس وانكسار الموجة بمنطقة الدراسة.
- تطبيق نموذج رياضي عن حركة التيارات البحرية بمنطقة العمل.
- نمذجة أثر عملية سحب المياه للنافورة من البحر وإعادة ضخه للبحر ثانية.

وأسفرت نتائج تلك الدراسة عن الآتى:

- الموقع المزمع تثبيت النافورة به مناسب، نظرًا لأن الطاقة الناتجة عن حركة الأمواج بالخليج ضعيفة، ولا تؤثر على جسم النافورة.

- اقتراح مكان آخر بديل لإقامة النافورة يعتبر أكثر أمانًا من المكان المقترح.
- الأثر البيئى الناشىء عن عملية الإنشاء والتثبيت ضعيفًا، ولا يكون إلا خلال فترة الإنشاء فقط.
- ستضيف عملية إنشاء النافورة أثرًا جماليًا للخليج الذى يعتبر منطقة سياحية جاذبة.